

Critical currents in vicinal $\text{YBa}_2\text{Cu}_3\text{O}_{7-\delta}$ films

J. H. Durrell,* G. Burnell, Z. H. Barber, M. G. Blamire, and J. E. Evetts

Department of Materials Science and Metallurgy, University of Cambridge, Pembroke Street, Cambridge, CB2 3QZ, UK.

(Dated: July 9, 2004)

Most measurements of critical current densities in $\text{YBa}_2\text{Cu}_3\text{O}_{7-\delta}$ thin films to date have been performed on films where the c -axis is grown normal to the film surface. With such films, the analysis of the dependence of j_c on the magnetic field angle is complex. The effects of extrinsic contributions to the angular field dependence of j_c , such as the measurement geometry and disposition of pinning centres, are convoluted with those intrinsically due to the anisotropy of the material. As a consequence of this, it is difficult to distinguish between proposed FLL structure models on the basis of angular critical current density measurements on c -axis films. Films grown on mis-cut (vicinal) substrates have a reduced measurement symmetry and thus provide a greater insight into the critical current anisotropy. In this paper previous descriptions of the magnetic field angle dependence of j_c in $\text{YBa}_2\text{Cu}_3\text{O}_{7-\delta}$ are reviewed. Measurements on $\text{YBa}_2\text{Cu}_3\text{O}_{7-\delta}$ thin films grown on a range of vicinal substrates are presented and the results interpreted in terms of the structure and dimensionality of the FLL in $\text{YBa}_2\text{Cu}_3\text{O}_{7-\delta}$. There is strong evidence for a transition in the structure of the flux line lattice depending on magnetic field magnitude, orientation and temperature. As a consequence, a simple scaling law can not, by itself, describe the observed critical current anisotropy in $\text{YBa}_2\text{Cu}_3\text{O}_{7-\delta}$. The experimentally obtained $j_c(\theta)$ behaviour of YBCO is successfully described in terms of a kinked vortex structure for fields applied near parallel to the a - b planes.

I. INTRODUCTION

As in all Type-II superconductors it is the structure and pinning behaviour of the Abrikosov lattice of flux vortices that determines the critical current properties of $\text{YBa}_2\text{Cu}_3\text{O}_{7-\delta}$ (YBCO). A comprehensive understanding of this is therefore an essential prerequisite to the development of technologically useful applications of this material. Low-temperature superconductors are either isotropic or slightly anisotropic¹. In contrast the more recently discovered high temperature superconductor (HTS) materials are all layered, strongly anisotropic materials. Superconductivity is associated with the cuprate planes which lie in the a - b planes of these materials. For the case of YBCO the Ginzburg-Landau anisotropy parameter, γ , is 5-7, whereas in $\text{Bi}_2\text{Sr}_2\text{CaCu}_2\text{O}_{8+x}$ (BSCCO 2212) the value is ~ 200 . This large difference has been attributed to the cuprate chains found along the b -axis between the cuprate planes in YBCO^{2,3,4} which may exhibit superconductivity.

For the more strongly anisotropic HTS materials it is reasonable to start by approximating them as two-dimensional superconductors with purely Josephson coupling between the superconducting layers⁵. This is the two dimensional superconductor described by Lawrence and Doniach⁶. This approach does not suffice for the case of YBCO. Indeed, over a wide range of applied field angles it appears that the flux lines in YBCO are the elliptical vortices which would be expected from anisotropic Ginzburg-Landau theory^{7,8}. For fields applied nearly parallel to the a - b planes Blatter *et al.*⁹ have predicted that there is a transition to a kinked vortex state where the contiguous vortex lines consist of alternating vortex string and pancakes segments parallel and perpendicular to the a - b planes. Measurements on single crystals indicate that the vortex lines only fully 'lock-in' to the planes when the field is within approximately 0.2° of the a - b planes¹⁰. The fully locked-in state will only be seen therefore in very perfect crystals.

The variation of the structure of individual flux lines as the

magnetic field direction changes with respect to the a - b planes means that no single scaling law will describe the magnetic field angle dependence of the superconducting properties of YBCO. The presence of anisotropic pinning centres will further complicate the observed behaviour. In order to elucidate the several contributions to the observed dependence of critical current on applied magnetic field angle it is necessary to reduce the measurement symmetry, ideally by arranging that the Lorentz force is not directed along a crystallographic axis. In this study we achieve this aim by employing YBCO thin films grown on mis-cut (vicinal) substrates. Thin films grown on single crystal substrates are a convenient experimental system especially since the step-flow growth favoured on vicinal substrates can lead to a very clean microstructure.

II. THEORY

There has been extensive earlier work on the angular dependence of critical currents in thin film YBCO. However these studies have all employed c -axis orientated films which greatly complicates the interpretation of the data obtained.

The first report of the nature of the variation of critical current with applied magnetic field angle was by Roas and co-workers¹¹. Although the angular resolution of their data was poor they identified the two most prominent features found in the $j_c(\theta)$ behaviour of YBCO, where θ is the angle between the applied field and the a - b planes. When the field is applied parallel to the a - b planes they observed an 'intrinsic pinning' peak which was attributed to pinning by the layered structure of the superconductor. Additionally a smaller peak was seen when the field was aligned parallel to the c -axis. This peak was associated by Roas *et al.* with pinning by twin planes. It is important to note that in their experiment the field was rotated in a plane perpendicular to the current so as to keep $j \wedge B$ maximized. If the field is swept in a plane containing the current direction the peak in the critical current observed

at $\theta = 0$ is due to the 'force-free'¹² effect.

It is immediately useful to note that these three peaks arise for entirely different reasons. The 'intrinsic' pinning peak is simply due to the anisotropy of the superconductor itself and the 'force-free' peak arises as the Lorentz force $j \wedge B$ tends to zero. It has since been shown that the primary source of pinning in c -axis films is due to dislocations at the edge of growth grains¹³. It is these dislocations that lead to the c -axis peak since they are most effective as pinning centres when the applied field is aligned with them. While the 'intrinsic' peak will not be expected to be sample dependent, the c -axis peak will depend on the film microstructure. This is supported by the wide variation in the prominence of the c -axis peak seen in different samples.

The nature of the 'intrinsic' peak is not straightforward. Similar behaviour is observed in BSCCO 2212 which can be quite satisfactorily described as a two dimensional superconductor. In BSCCO 2212 the flux lines take the form of stacks of pancake vortices localized within the a - b planes¹⁴. A consequence of this is that any angular dependent behaviour can be taken as depending entirely on the c -axis component of the applied field, the 'Kes law'¹⁵. In small fields the vortex structure does, however, show more complex behaviour¹⁶. The 'Kes law' has been found to agree very well with experiment in BSCCO 2212¹⁷. Although Jakob *et al.*¹⁸ reported that this scaling law also worked well for the case of YBCO, close examination of their data shows that while the fit for BSCCO is indeed very good, the correlation is much less satisfactory for YBCO. Moreover a consequence of the Kes law is that BSCCO 2212 will not exhibit a 'force-free' effect¹² as the local field is not aligned with the current direction, whatever the orientation of the external field. This is experimentally observed as constant critical current when the applied magnetic field is rotated about the c -axis¹⁹ with a constant angle between the field and the a - b planes. YBCO does exhibit such an enhancement of critical current in the 'force-free' geometry^{8,20,21}. YBCO cannot, therefore, be treated as approximating to a two dimensional superconductor.

Tachiki and Takahashi²² considered the effect of layering in YBCO by noting that for $T < 70$ K the core size for a vortex lying along the a - b plane is less than the inter-planar spacing. They extended their model to cover orientations other than aligned along the a - b plane by envisaging kinked vortex lines consisting of locked-in vortex segments connected by short lengths crossing the cuprate planes²³. Although some authors found their data broadly fitted their predictions^{24,25,26} none found the predicted lock-in plateau²⁷. This is in all likelihood because the lock-in angle is small 0.2° and is suppressed by only slight imperfections in the crystal structure. The lock-in effect is however seen in high quality single crystals¹⁰.

The intrinsic pinning peak does not disappear at higher temperatures where the vortex core is larger than the interlayer spacings. If the superconductor is simply considered as being anisotropic, Ginzburg-Landau theory predicts that the vortex cores will become progressively more elliptical as the field is tilted. This may be described by considering an angle dependent mass anisotropy parameter^{1,7} ϵ_θ . This parameter is given by $\epsilon_\theta^2 = \epsilon^2 \cos^2 \theta + \sin^2 \theta$ where ϵ is the mass anisotropy pa-

rameter, $\epsilon = 1/\gamma = \sqrt{\frac{m_{ab}}{m_c}}$. From this, scaled versions of various experimental parameters may be obtained, for example $B_{c2}(\theta) = B_{c2}/\epsilon_\theta$. For the case of a tilted vortex line parallel to the a - b planes the vortex core size in the c direction is reduced to $\epsilon_\theta \xi_{ab}$, where ξ_{ab} is the G-L coherence length in the a - b planes. If it is assumed that the smaller core is more effectively pinned, then an 'intrinsic' pinning peak will still be found. The expected angular dependence for j_c ,

$$j_c(B, \theta) = j_c(\epsilon_\theta B, \theta = 90^\circ) \quad (1)$$

is not straightforward as, in general, j_c does not depend on B in a simple fashion. Divergence from this expected behaviour at a particular angle, θ , can however reasonably be used to infer the existence of anisotropic pinning, as has recently been discussed by Civalé *et al.*²⁸

Blatter *et al.*⁹ reconciled these various ideas by proposing the existence of a cross-over from a lattice of conventional rectilinear, but anisotropic, Abrikosov vortices to a regime of kinked vortices, similar to the Tachiki and Takahashi model. In the kinked regime pancake vortices in the cuprate planes are linked by Josephson string vortices in the interlayers. The pancake vortices have a fully developed normal core of extent ξ_{ab} . The vortices lying between the cuprate planes are Josephson in nature and do not exhibit full suppression of the superconducting order parameter.

Blatter introduced two critical angles, θ_1 and θ_2 . Defining $\theta = 0$ to be when the applied field is aligned with the cuprate planes for $\theta > \theta_1$ the flux lines are conventional straight Abrikosov vortices. For $\theta_1 > \theta > \theta_2$ the flux vortices are distorted towards the kinked state whilst for $\theta < \theta_2$ the kinked state is fully formed. They express θ_1 as

$$\tan(\theta_1) = \frac{d}{\xi_{ab}(t)} \quad (2)$$

t is the reduced temperature (T/T_c), d is the interlayer spacing and T_c is the superconducting transition temperature. The second critical angle θ_2 is expressed as

$$\tan(\theta_2) = \epsilon \quad (3)$$

Above a certain critical temperature T_{cr} the transition is expected to be suppressed and rectilinear Abrikosov vortices are seen for all orientations of applied magnetic field. This critical temperature is defined as being that at which $\xi_{ab}(T_{cr}) = d/\sqrt{2}$. In YBCO these values are²⁹ $\theta_1 \sim 35^\circ$ and $\theta_2 \sim 11^\circ$ for $t=0$. T_{cr} is predicted to be about 80 K. From Eq. 3 we may deduce that θ_2 will depend only weakly on temperature since $\epsilon = \xi_c/\xi_{ab}$ and both ξ_{ab} and ξ_c have a similar temperature dependence.

As would be expected, the Josephson string vortices localized within the a - b planes are more weakly pinned than the pancake vortices²¹. In spite of this, a vortex channelling effect cannot be seen in c -axis films since there is never a component of the Lorentz force directed in the weakly pinned direction. In the reduced symmetry found in measurements on vicinal films the expected intrinsic vortex channelling effect is observed^{29,30}. As predicted from Eq. 2 the width of

the vortex channelling effect has been shown to vary with changing superconducting anisotropy in calcium doped and de-oxygenated YBCO films³¹.

III. EXPERIMENTAL TECHNIQUE

Thin films of $\text{YBa}_2\text{Cu}_3\text{O}_{7-\delta}$ were prepared by pulsed laser deposition. The films all had thicknesses of between 100 and 200 nm and were grown on single crystal SrTiO_3 substrates mis-cut by an angle, θ_v , towards the (001) direction. Vicinal films of YBCO prepared on mis-cut substrates typically exhibit 'step-flow' growth which leads to a terraced structure with the terraces perpendicular to the miscut^{32,33,34,35,36}. It should be noted that the films had a low density of anti-phase boundaries and stacking faults, this was confirmed by HREM studies³⁰. These types of defects disrupt the a - b planes and make the interpretation of observed critical current in terms of the FLL structure and anisotropy impossible. Such defects, when present, do however strongly increase the observed critical current^{37,38,39}. The different growth modes of YBCO films on vicinal substrates have been recently discussed by Maurice *et al.*³⁶

Current tracks were patterned by photo-lithography and Ar-ion milling to allow four terminal IV measurements, the tracks were $200 \times 10 \mu\text{m}$ between the voltage contacts and were patterned both perpendicular (**T**) and parallel (**L**) to the vicinal step direction³³. Contacts were prepared by sputtering Ag/Au bi-layers. The samples were characterized using a two-axis goniometer⁴⁰ mounted in an 8 T magnet. The geometry of the measurement, for a **T** track is shown in Fig. 1.

An IV curve was recorded at each set of experimental parameters (B, T, θ, ϕ). Critical current values were determined from these curves using a criterion of $0.5 \mu\text{V}$. The choice of a voltage criterion to determine critical current, I_c from IV curves is arbitrary, this value was chosen as the lowest practical value given the noise in the experiment. It was noted that the overall form of all the observed j_c characteristics did not change when the saved IV characteristics were reanalyzed with different voltage criteria.

IV. EXPERIMENTAL RESULTS

In order to provide a fuller characterization of the $j_c(\theta)$ behaviour in vicinal films, and in particular the vortex channelling effect first reported by Berghuis *et al.*²⁹, $j_c(T, B, \theta, \phi)$ studies were performed on YBCO films grown on substrates with varying mis-cut angles. The data presented in this article were all obtained on (**T**) tracks, since it is only in this geometry that the vortex channelling effect is observed. This occurs since there is no Lorentz force component in the weakly pinned direction on the vortex strings in measurements on (**L**) tracks.

Fig. 2 shows data taken in a 1 T field for a range of temperatures on a 10° vicinal film. The vicinal channelling minimum is prominent and as expected disappears above 80K

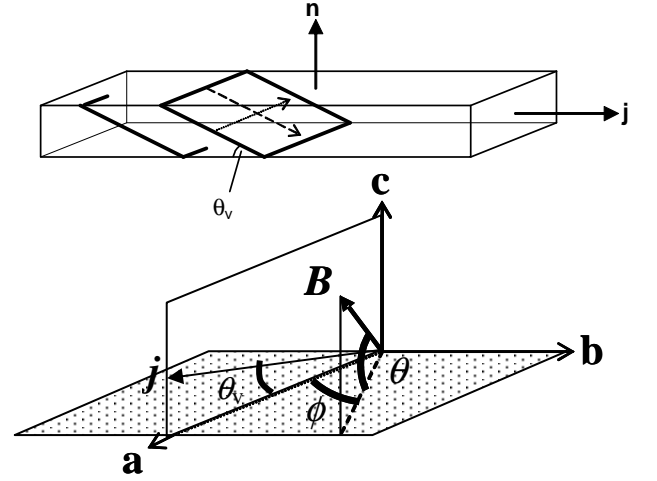


FIG. 1: Geometry of the measurement of a **T** track. The upper part of the figure shows the orientation of the a - b planes with respect to the surface of the film. The mis-cut (vicinal) angle of the substrate is given by θ_v . The lower part indicates how the tilt angle θ and rotation angle ϕ specify the orientation of the external magnetic field. $\theta=0$ is defined as when the field is parallel to the planes. At $\theta = \theta_v$ $\phi=0$ the field is aligned with the current.

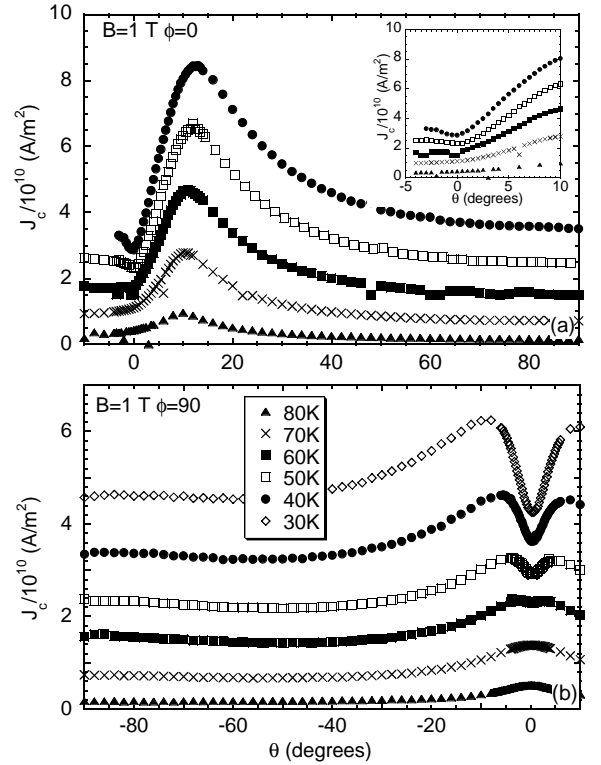


FIG. 2: j_c data taken on a **T** track patterned on a YBCO film grown on a 10° mis-cut substrate. The upper $j_c(\theta)$ plot (a) was obtained with $\phi = 0^\circ$ and in a 1 T field, the inset shows an enlargement of the channelling minimum. The lower plot (b) was obtained with $\phi = 90^\circ$. The vortex channelling effect is visible in both plots, in (a) the peak arises from the force free geometry whilst in (b) the peak which is partly suppressed by channelling arises from intrinsic pinning.

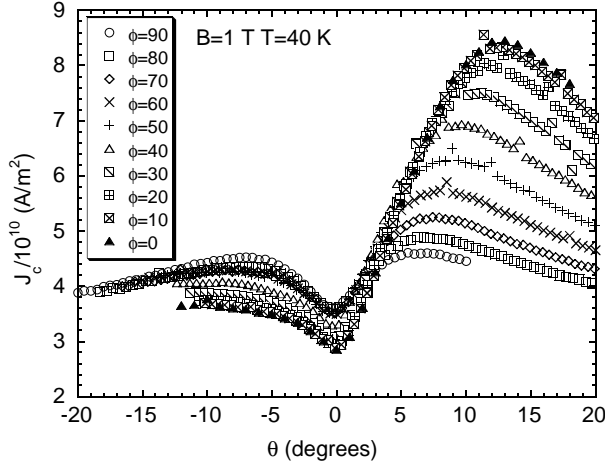


FIG. 3: $j_c(\theta)$ near the vortex channelling minimum, at 1 T, 40 K and varying values of ϕ , for a YBCO film grown on a 10° mis-cut substrate.

(T_{cr}) when the flux lines are conventional Abrikosov vortices for all field orientations²⁹.

In Fig. 2a, with $\phi=0$ the channelling minimum, corresponding to the field being aligned with the a - b planes, is offset by 10° from a peak in j_c , which corresponds to the 'force-free' orientation. This confirms that the superconducting film indeed has its c -axis offset by 10° with respect to the surface normal. In Fig. 2b where θ is swept with $\phi=90^\circ$ the channelling minimum can be seen to be coincident with the intrinsic peak in j_c which is consequently suppressed. The channelling minimum is seen for all ϕ values, as is shown in Fig. 3. The critical current of the minimum can be seen to be higher at $\phi=90^\circ$ than at $\phi=0^\circ$ when $\theta=0^\circ$. Although both $\theta=0^\circ, \phi=0^\circ$ and $\theta=0^\circ, \phi=90^\circ$ are orientations of the magnetic field that give rise to vortex channelling, in the former case the Lorentz force is purely directed along the a - b planes whereas in the latter case there is a component directed along the c -axis as well.

It proved impossible to grow good quality vicinal films with a clean microstructure for angles greater than 10° . In such films no channelling effect was observed. This is probably due to growth no longer being perfectly epitaxial, this will give rise to dislocations³⁷, stacking faults and anti-phase boundaries³⁹ extending through the film. Such defects will suppress in-plane vortex channelling³⁰.

Similar data sets were also obtained on 2° and 4° vicinal films. $j_c(\theta)$ data obtained on 4° films is shown in Fig. 4 with varying T at 1 T and in Fig. 5 with varying B at 60 K. As in the case of the film grown on a 10° mis-cut substrate we observe minima due to vortex channelling in both geometries. As before at higher temperatures the channelling is less pronounced.

The variation of the $j_c(\theta)$ behaviour with field is shown in Fig. 5. In the $\phi=0^\circ$ geometry the effect of vortex channelling is clear and the overall form of the minimum does not change with varying field, being very sharp. In the $\phi=90^\circ$ geometry however the channelling effect is not very pronounced, and

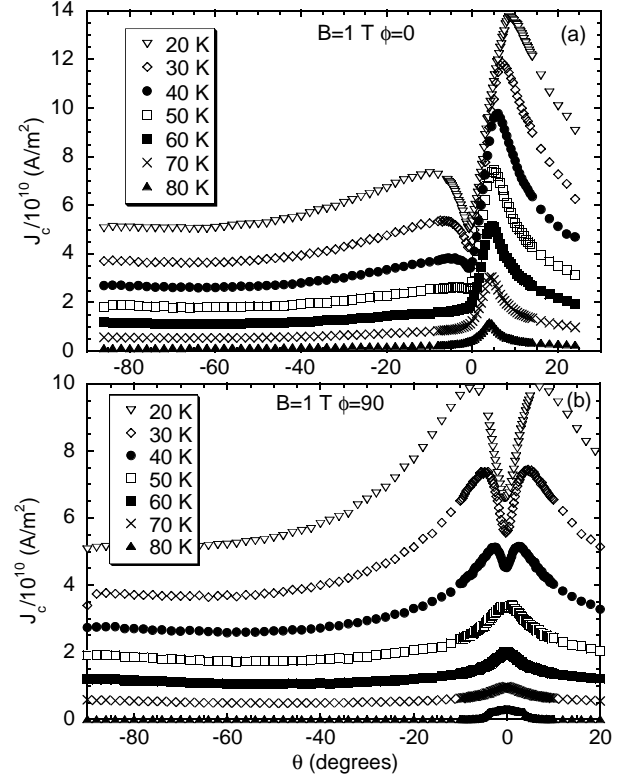


FIG. 4: Critical current, j_c versus field tilt, θ , data recorded at 1 T and varying temperature on an YBCO film grown on a 4° mis-cut substrate. In (a) ϕ was set to 0° and in (b) 90° .

the minimum is less distinct. As the intrinsic pinning peak and the vicinal channelling minimum are superposed this is a function of the relative strengths of the two effects.

Even with a small mis-cut of 2° it is possible to obtain vicinal growth and consequently observe vortex channelling. This is shown in Fig. 6. The close angular proximity of the vortex channelling minimum and the force-free peak mean that the critical current increases by a factor of five between $\theta=-2^\circ$ and $\theta=0$. As the minimum due to vortex channelling and the force free effect are overlapping the point of maximum j_c is shifted. This is also visible to a lesser extent in data recorded on the other vicinal angles. Measurements were not performed on substrates with mis-cuts less than 2° , it is expected however that the vortex channelling effect only disappears when the mis-cut angle is small enough that the growth becomes the c -axis island growth typically seen in YBCO thin films.

In summarizing the experimental results it is possible to make several general observations. The vicinal channelling effect described in²⁹ in films grown by sputtering has been reproduced in films grown by pulsed laser deposition. This tends to suggest strongly that the effect is intrinsic rather than linked to a particular growth technique. This channelling effect will therefore be seen in any YBCO sample where the current is not directed along the a - b planes and the crystal structure is free of defects that disrupt the continuity of the a - b planes³⁰. The channelling effect extends over a range of miscut angles, the upper limit being due to the difficulty of

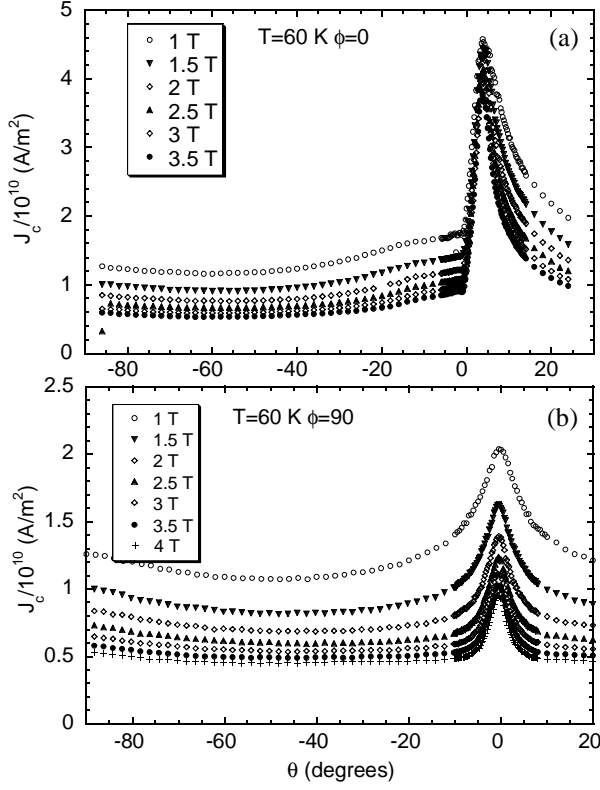


FIG. 5: Critical current, j_c versus field tilt, θ , data recorded at 60 K and varying field on an YBCO film grown on a 4° mis-cut substrate. In (a) ϕ was set to 0° and in (b) 90° .

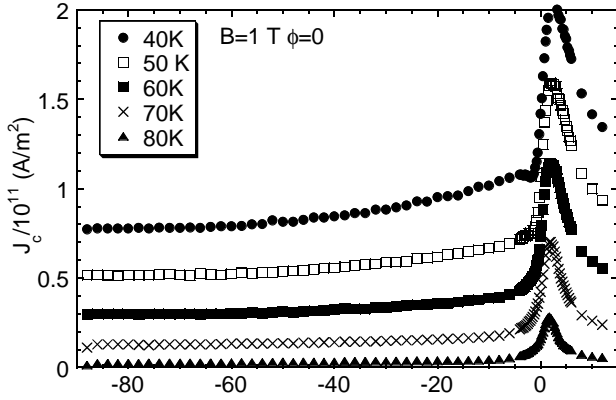


FIG. 6: Critical current, j_c versus field tilt, θ , data recorded at 1 T and varying temperature on an YBCO film grown on a 2° mis-cut substrate, ϕ was set to 0° .

getting epitaxial growth on substrates with a large angle of mis-cut. As previously observed channelling is suppressed at high temperatures irrespective of the mis-cut angle. Moreover the effect is most easily seen in the $\phi = 0$ configuration where the channelling minimum is off-set from the 'force-free' peak.

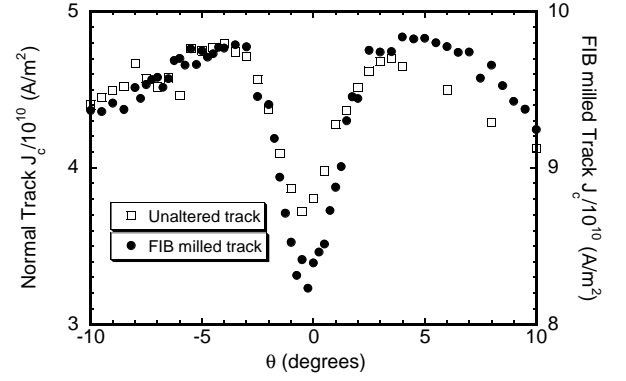


FIG. 7: The vortex channelling minimum measured on a 10 micron wide track in a 6° vicinal film at $\phi = 90^\circ$ before (open squares) and after (closed circles) thinning to $\approx 2 \mu\text{m}$ using a focussed ion beam microscope.

V. TRACK WIDTH

In this article we seek to identify the extent of the channelling minimum with the angular range in which there is a cross-over from rectilinear Abrikosov to kinked string-pancake vortex lines. To support this argument it is necessary to exclude the possibility that the width of a particular current track has an effect on the channelling minimum by changing the length of a - b plane into which a vortex line need align to lock-in. This will be more pronounced in the $\phi = 90^\circ$ geometry where the vortex line must align with the $10 \mu\text{m}$ width of the current track.

In the $\phi = 90^\circ$ geometry the channelling minimum was measured on a 6° vicinal film on a $10 \mu\text{m}$ wide track. The track was subsequently thinned in a focussed ion beam microscope to a width of $2 \mu\text{m}$. The thinned track was subsequently re-measured. As gallium ions, used in the milling process, can have a deleterious effect on YBCO the T_c of the sample was checked and seen to have remained the same. The milling was carried out in such a way as to minimise the amount of gallium spread over the surface of the sample.

The results from this investigation are shown in Fig. 7. It can be seen that the width of the channelling minimum is unaffected. The variation in the absolute value of the critical current may be partly due to uncertainty in the width of the superconducting channel, the region around a cut made with a gallium beam will also have suppressed superconductivity due to gallium implantation. This measurement clearly demonstrates therefore that the width of the measurement track does not affect the width of the j_c minimum associated with vortex channelling.

VI. DISCUSSION

The existence of a vortex channelling effect in measurements on vicinal YBCO films is clear from the series of experiments presented in this article. In this section the magnetic field orientation at which cross-over from Abrikosov vortices

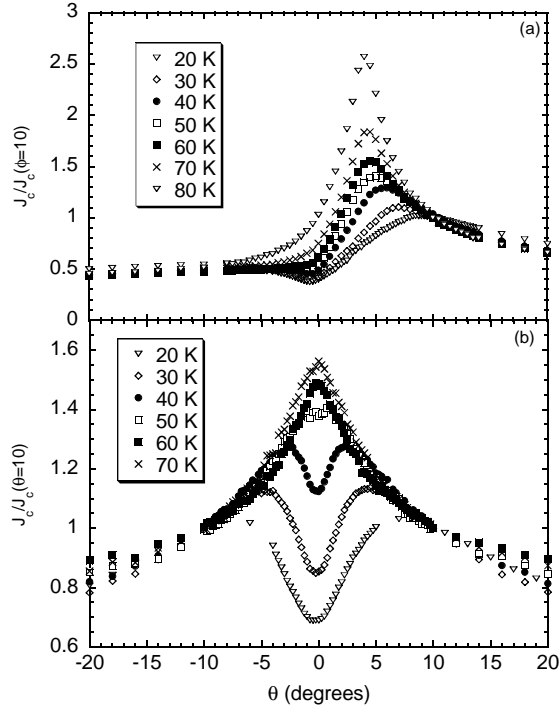


FIG. 8: Data from Fig. 4 plotted against $j_c/j_c(\theta = 10^\circ)$. ($\theta_v = 4^\circ$)

to the kinked configuration occurs will be determined. The form of the channelling minimum will be modelled by considering the Lorentz forces and pinning on the separate vortex elements.

As has been discussed previously the scaling law described in Eq. 1 is not expected to work particularly well over the entire angular range where the vortices are conventional in nature. This is primarily due to enhanced pinning at $\theta = 0^\circ$ from twins and dislocations. However, away from both this enhanced extrinsic pinning and the cross-over into the kinked vortex state the primary contribution to $j_c(\theta)$ is not unreasonably expected to arise primarily from the anisotropy of the material. In Fig. 8 the $j_c(\theta)$ characteristic with varying temperature from Fig. 4 is shown plotted as $j_c(\theta)/j_c(\theta = 10^\circ)$. If the scaling law applies temperature should not change the form of the rescaled curves.

From the figure this does indeed seem to be the case outside the range where the behaviour crosses over into the vicinal channelling regime. In Fig. 8 the region over which the $j_c(\theta)$ plots diverge has a range of about 20° , this is consistent with the prediction of Eq. 3 since θ_2 depends only on the ratio between the a - b plane and c -axis coherence lengths. In Fig. 8b all the peaks follow the same form with the position of the crossover into the channelling minimum appearing to depend on temperature.

Given that the $j_c(\theta)$ characteristic cannot be described in terms of the simple G-L scaling equation given in Eq. 1 it is important to determine if the behaviour near $\theta = 0^\circ$ is consistent with kinked vortex lines. If the vortex lines are indeed kinked it should be possible to predict the $j_c(\theta)$ behaviour by considering the Lorentz forces and pinning on the two types

vortex segment, vortex strings and pancakes.

In the $\phi = 0^\circ$ case the external field direction lies parallel to the current flow for $\theta = \theta_v$ and is tilted toward the c -axis as θ is varied. For an individual rectilinear vortex line the Lorentz force is given by $j_c \times \Phi_0 = f_L$ where f_L is the Lorentz force per unit length on a vortex line. At the critical current f_L is simply equal to f_p , the pinning force per unit length. This analysis assumes the pinning forces arise from strong pinning centres. In this limit the collective pinning volume is that of a single vortex and it is reasonable to consider pinning forces acting on individual vortex lines. In the case of a kinked vortex line the Lorentz forces on and the pinning of the separate segments will be different. For a kinked vortex line spanning two points l apart and at an angle θ to the a - b planes there will be a length $l_p = l \sin \theta$ of pancake elements and $l_s = l \cos \theta$ of string elements. Where the vicinal angle is θ_v the Lorentz force on the entire line per unit length will be (the Lorentz forces in this geometry being in the same direction on both elements):

$$f_L = j\phi_0(\cos \theta \sin \theta_v - \sin \theta \cos \theta_v) \quad (4)$$

Immediately it can be seen that even a kinked vortex line will experience a force free effect since at $\theta = \theta_v$ f_L will be zero. This is indeed what is experimentally observed, however experimentally the critical current does not become infinite. There will therefore be two regimes for angle dependence of the critical current in the kinked vortex regime. One will apply where dissipation arises from the vortices depinning, the second will arise in the regime near the force free orientation where a different dissipative mechanism must apply.

The pinning force available on the vortex lines maybe calculated by considering pinning on individual string and pancake elements. The pinning force per unit length of vortex opposing the motion of the vortices will be given by:

$$f_p = f_{p, str} \cos \theta + f_{p, pc} \sin \theta \quad (5)$$

where the subscript 'pc' refers to forces on vortex pancakes and 'str' to those on vortex strings. At $j = j_c$ $f_p = f_L$ so we may write the following equation for $j_c(\theta)$ combining Eqs. 4 and 5:

$$j_c = \frac{f_{p, str} \cos \theta + f_{p, pc} \sin \theta}{\phi_0(\cos \theta \sin \theta_v - \sin \theta \cos \theta_v)} \quad (6)$$

The fit of the model to data on a 4° miscut samples at 40K and 1 T is shown in Fig. 9, here $f_{p, pc}$ is $8.1 \times 10^{-5} \text{ Nm}^{-1}$ and $f_{p, str}$ is $4.9 \times 10^{-6} \text{ Nm}^{-1}$. The model, with simply two parameters, reproduces the main features of the experimentally observed behaviour, however it predicts an infinite critical current when the current is aligned with the field since, as discussed above, at this point the Lorentz forces on the string and pancake segments are opposite and balance out. Three regions may be identified; in the first the flux lines are rectilinear but anisotropic, in the second the vortices are kinked but depin conventionally and in the third regime around the 'force-free' geometry the critical current must arise from an alternative mechanism.

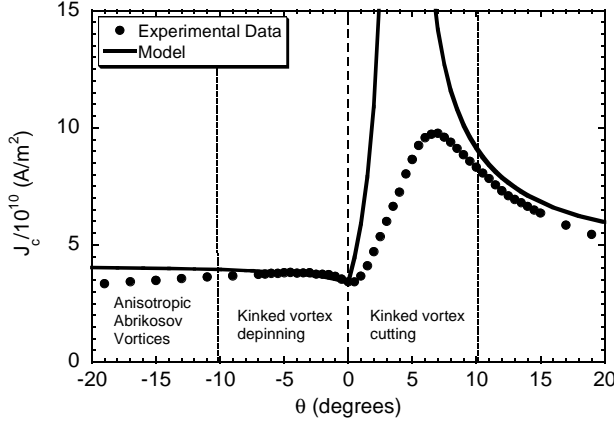


FIG. 9: Comparison of the model treating the pinning on individual vortex segments to experimental data in the $\phi=0^\circ$ orientation. The experimental data was taken on a 4° vicinal film at 1 T and 40K. The dotted lines indicate θ_2 and the dashed line the point at which the direction of the Lorentz force on the string segments reverses direction.

In this distinct regime, which extends between $\theta = 0^\circ$ and slightly beyond the 'force free' orientation where $\theta = \theta_v$, a different mechanism must account for the finite critical current. In this range the Lorentz forces on the vortex string and pancake segments are in opposite directions. The vortex pancakes are strongly pinned and subject to only a small force per unit length. It is likely, therefore, that dissipation occurs through cutting and joining with adjacent vortices when each string segment is subject to a large enough force. Flux cutting processes have been described by several authors, it is important to note that at no time in the phase slip process does a 'free' vortex end appear^{12,41,42,43,44}.

If a single vortex string segment is considered it will be subject to certain Lorentz force, which will be opposed by the elastic tension in the vortex string as it is deformed and by the pinning force on the vortex string. When the force on the vortex string exceeds a certain value, f_{cut} the vortex string cuts and joins. This force represents therefore the critical current condition. A similar mechanism has been identified in grain boundaries in YBCO, which is another system in which vortex channelling is found⁴⁵.

Taking a single vortex string in the $\phi = 0^\circ$ geometry the Lorentz force on the vortex string segment will be given by $f_{L,seg} = j_c \phi_0 d \sin \theta_v \cos \theta / \sin \theta$. The length of an individual vortex segment for a particular magnetic field tilt is given by $d / \sin \theta$, where d is the spacing between cuprate planes. In YBCO d is one third of the c -axis lattice parameter ≈ 0.39 nm. The available pinning is given by $f_{p,seg} = f_{cut} + (f_{p,str} d / \sin \theta)$ where f_{cut} is the force required on a single segment for cutting and cross-joining to occur. Combining these we may write the following equation for the θ dependence of the critical current in the vortex cutting region.

$$j_c = \frac{1}{\phi_0} \left[\frac{f_{cut} \tan \theta}{d \sin \theta_v} + \frac{f_{p,str}}{\sin \theta_v \cos \theta} \right] \quad (7)$$

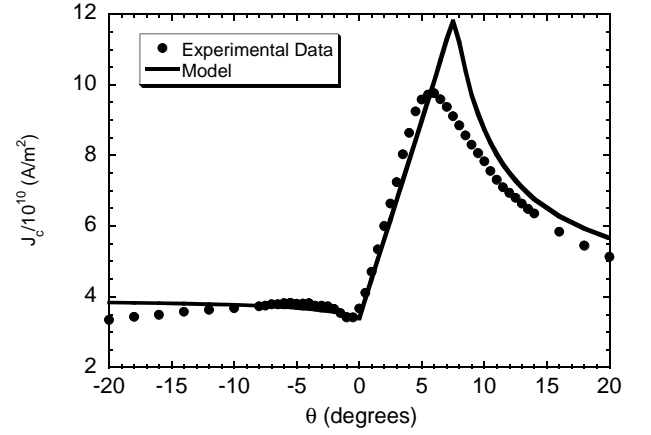


FIG. 10: The figure shows the behaviour predicted by extending the model shown in Fig. 9 to take account of vortex cutting when the Lorentz forces on the string and pancake segments are in opposite directions. The experimental data was taken on a 4° vicinal film at 1 T and 40K.

The actually observed critical current behaviour for a kinked vortex will be the lower of that predicted by Eqs. 6 and 7 for any particular value of θ . This simply because flux flow occurs if it requires a smaller Lorentz force than that required for the cutting process. If the simple assumption is made that the cutting force required per segment is independent of its length choosing a cutting force of 3.6×10^{-14} N for the 40 K and 1 T data shown in Fig. 9 results in a reasonable fit to the experimental data. This is shown in Fig. 10.

It is clear therefore that there is a region between $\theta = 0^\circ$ and $\theta \approx \theta_v$ where the flux flows by cutting and cross joining rather than by depinning entire vortex lines. Treating the flux cutting force per segment as being independent of length appears to be a reasonable first approximation.

A similar approach may be used to model the behaviour of the θ dependence of the critical current in the $\phi = 90^\circ$ orientation by separately considering the forces on the string and pancake vortex segments. Here the field is tilted so that the flux lines are always perpendicular to the current. The force on the vortex strings will be directed normal to the plane of the film while the forces on the pancake segments is directed along the a - b planes. The strong intrinsic pinning means that the component of the force on the vortex strings directed out of the a - b planes is always opposed by an equal pinning force and the forces need only be resolved within the plane. A section of a tilted vortex line is shown in Fig. 11. The component of the force on the strings within the a - b plane per unit length is given by $j \Phi_0 \cos \theta \sin \theta_v$. The force per unit length on the vortex pancakes is given by $j \Phi_0 \sin \theta \cos \theta_v$, the $\cos \theta_v$ factor arising from the fact the the pancake segments are not perpendicular to the current. The resulting force per unit length on the vortex is then:

$$f_L = j_c \phi_0 \sqrt{(\cos \theta \sin \theta_v)^2 + (\sin \theta \cos \theta_v)^2} \quad (8)$$

The pinning force will act in the opposite direction to this force with the pancake pinning per unit length given by

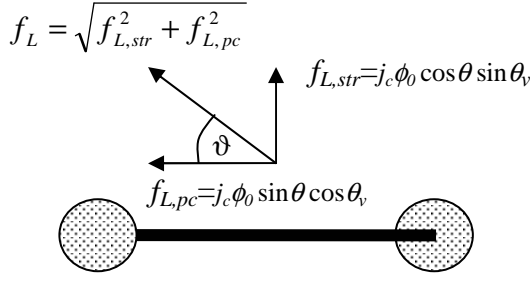


FIG. 11: Schematic of the forces on a segment of kinked vortex line, the c -axis is perpendicular to the page. The figure shows, schematically, a vortex string connecting two vortex pancakes. One pancake will lie in the cuprate plane above the string the other in the cuprate plane below it. The angle ϑ describes the rotation of the resolved force on the vortex string within the a - b planes. Forces directed outside the a - b plane may be neglected as strong intrinsic pinning restricts the motion of vortex segments in the c -axis direction.

$$j_c = \frac{1}{\phi_0} \left(\frac{f_{p,pc} \sin \theta}{\sqrt{(\cos \theta \sin \theta_v)^2 + (\sin \theta \cos \theta_v)^2}} + \frac{f_{p,str} \cos^2 \theta \sin \theta_v}{(\cos \theta \sin \theta_v)^2 + (\sin \theta \cos \theta_v)^2} \right) \quad (9)$$

Using Fig. 9 it is possible to compare this model for the θ dependence of the critical current to experimental data. A comparison to data obtained on a 4° vicinal film at 40 K and 1 T is shown in Fig. 12. Within the region for which the model is expected to be valid, $|\theta| < \theta_2$ a good fit to the experimental data is obtained with $f_{p,pc} = 8.1 \times 10^{-5} \text{ Nm}^{-1}$ and $f_{p,str} = 6.2 \times 10^{-6} \text{ Nm}^{-1}$. This is the same pancake pinning force as the $\phi = 0^\circ$ geometry but the required string pinning force is marginally higher. One possible source of this discrepancy may be that only the force balance in the a - b plane has been considered. The vortex strings are also subject to a Lorentz force which tends to push them in the c -axis direction, this may increase the pinning force against movement in the a - b plane.

VII. CONCLUSION

In the high T_c superconductor $\text{YBa}_2\text{Cu}_3\text{O}_{7-\delta}$ there is a temperature and magnetic field orientation dependent crossover from a lattice of rectilinear Abrikosov flux lines to a lattice of 'kinked' vortices. These kinked vortex lines consist of vortex pancakes crossing the cuprate planes and Josephson strings aligned in the charge reservoir layers.

As a consequence of this, 'intrinsic' vortex channelling is observed providing the superconducting transport current does not flow parallel to the a - b planes. The minima in the critical current versus magnetic field angle characteristic occurs not because the vortex lines are 'locked-in' to the a - b planes over a wide angular range but because the transition to the kinked vortex state changes the angular dependence of

$f_{p,pc} \sin \theta$. The string pinning force must take into account that the vortex string is only pinned for movement perpendicular to its length²¹ and will be given by $f_{p,str} \cos \theta \sin \vartheta$. From Fig. 11 we can see that orientation of the Lorentz within the a - b plane, ϑ will be given by $\tan \vartheta = f_{L,pc}/f_{L,str}$. We may therefore write the following equation for $j_c(\theta)$:

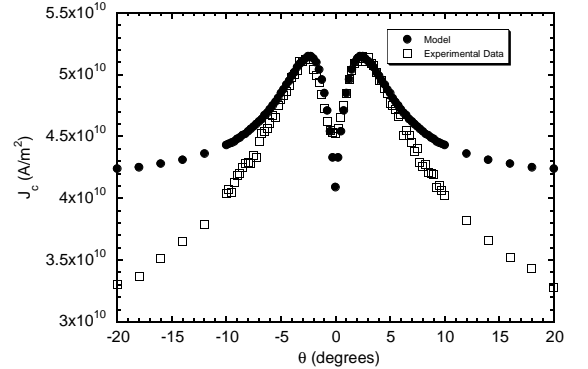


FIG. 12: Comparison of experimental data with the model prediction for an external magnetic field in the $\phi = 90^\circ$ geometry. The experimental data was taken on a 4° vicinal film at 1 T and 40 K.

the magnitude of the available pinning force. At the angle where the vortex lines are expected to align with the planes imperfections in the films and thermal activation probably ensure that the vortex lines are never entirely string like. We have shown that the angular dependence of the critical current in the 'kinked' range may, to a first approximation, be considered by summing the Lorentz force on the separate vortex elements and comparing this to the pinning force available to these elements. The vortex channelling effect arises because although vortex strings are strongly pinned for motion parallel to the c -axis they are comparatively weakly pinned for motion in the a - b planes.

In the regime where the forces on vortex pancakes and

strings are opposed it is apparent that a different mechanism serves to limit the critical current behaviour. We argue that it is cutting and cross joining of individual vortex string segments that give rise to flux flow. The vortex pancakes themselves do not flow in this region.

For magnetic fields well away from parallel to the a - b planes, the properties of the rectilinear vortices may be treated by using anisotropic Ginzburg-Landau theory to describe how these elliptical vortices interact with pinning centres. The $j_c(\theta)$ behaviour in thin films does not, however, scale using the simple scaling law obtained by Blatter *et al.* since the strong pinning found in such films is highly anisotropic.

The complexity of the angular variation of the vortex struc-

ture in $\text{YBa}_2\text{Cu}_3\text{O}_{7-\delta}$ is due to this material's relatively low superconducting anisotropy as compared to most other high T_c superconductors. The consequent cross over transitions in the vortex lattice make it impossible to apply a single scaling law to the angular dependence of the critical current.

Acknowledgments

This work was supported by the Engineering and Physical Sciences Research council.

-
- * Electronic address: jhd25@cam.ac.uk
- ¹ V. G. Kogan and J. R. Clem, in *Concise Encyclopedia of Magnetic and Superconducting Materials*, edited by J. E. Evetts (Pergamon, Oxford, 1992).
 - ² R. J. Cava, A. W. Hewat, E. A. Hewat, B. Batlogg, M. Marezio, K. M. Rabe, J. J. Krajewski, W. F. Peck, and L. W. Rupp, *Physica C* **165**, 419 (1990).
 - ³ L. F. Hou, J. Deak, P. Metcalf, and M. McElfresh, *Physical Review B* **50**, 7226 (1994).
 - ⁴ J. L. Tallon, C. Bernhard, U. Binniger, A. Hofer, G. V. M. Williams, E. J. Ansaldo, J. I. Budnick, and C. Niedermayer, *Physical Review Letters* **74**, 1008 (1995).
 - ⁵ J. R. Clem, *Superconductor Science and Technology* **11**, 909 (1998).
 - ⁶ W. E. Lawrence and S. Doniach, in *Proceedings of the 12th International Conference on Low Temperature Physics*, edited by E. Kanda (Keigaku, Tokyo, Kyoto, 1970), p. 361.
 - ⁷ G. V. Blatter, G. and A. Larkin, *Phys. Rev. Lett.* **68**, 875 (1992).
 - ⁸ R. Herzog, Ph.D. thesis, University of Cambridge (1997).
 - ⁹ G. Blatter, M. V. Feigelman, V. B. Geshkenbein, A. I. Larkin, and V. M. Vinokur, *Reviews Of Modern Physics* **66**, 1125 (1994).
 - ¹⁰ A. A. Zhukov, H. Kupfer, P. A. J. de Groot, and T. Wolf, *Journal of Low Temperature Physics* **117**, 1513 (1999).
 - ¹¹ B. Roas, L. Schultz, and G. Saemannishenko, *Phys. Rev. Lett.* **64**, 479 (1990).
 - ¹² A. M. Campbell and J. E. Evetts, *Advances in Physics* **50**, 1249 (1972).
 - ¹³ B. Dam, J. M. Huijbregtse, F. C. Klaassen, R. C. F. van der Geest, G. Doornbos, J. H. Rector, A. M. Testa, S. Freisem, J. C. Martinez, B. Stauble-Pumpin, et al., *Nature* **399**, 439 (1999).
 - ¹⁴ J. R. Clem, *Physical Review B* **43**, 7837 (1991).
 - ¹⁵ P. Kes, J. Aarts, V. Vinokur, and C. van der Beek, *Phys. Rev. Lett.* **64**, 1063 (1990).
 - ¹⁶ A. E. Koshelev, *Physical Review Letters* **83**, 187 (1999).
 - ¹⁷ P. Schmitt, P. Kummeth, L. Schultz, and G. Saemannishenko, *Physical Review Letters* **67**, 267 (1991).
 - ¹⁸ G. Jakob, M. Schmitt, T. Kluge, C. Tomerosa, P. Wagner, T. Hahn, and H. Adrian, *Physical Review B* **47**, 12099 (1993).
 - ¹⁹ J. H. Durrell, G. Gibson, Z. H. Barber, J. E. Evetts, R. Rössler, J. Pedarnig, and D. Bäuerle, *Applied Physics Letters* **77** (2000).
 - ²⁰ G. Ravi Kumar, M. R. Koblishka, J. C. Martinez, R. Griessen, B. Dam, and J. Rector, *Physica C* **235-240**, 3053 (1994).
 - ²¹ J. H. Durrell, R. Herzog, P. Berghuis, A. P. Bramley, E. J. Tarte, Z. H. Barber, and J. E. Evetts, *Superconductor Science and Technology* **12**, 1090 (1999).
 - ²² M. Tachiki and S. Takahashi, *Solid State Communications* **70**, 291 (1989).
 - ²³ M. Tachiki and S. Takahashi, *Solid State Communications* **72**, 1083 (1989).
 - ²⁴ T. Nishizaki, T. Aomine, I. Fujii, K. Yamamoto, S. Yoshii, T. Terashima, and Y. Bando, *Physica C* **185**, 2259 (1991).
 - ²⁵ T. Nishizaki, T. Aomine, I. Fujii, K. Yamamoto, S. Yoshii, T. Terashima, and Y. Bando, *Physica C* **181**, 223 (1991).
 - ²⁶ T. Aomine, T. Nishizaki, F. Ichikawa, T. Fukami, T. Terashima, and Y. Bando, *Physica B* **194**, 1613 (1994).
 - ²⁷ D. Feinberg and C. Villard, *Physical Review Letters* **65**, 919 (1990).
 - ²⁸ L. Civale, B. Maiorov, A. Serquis, J. O. Willis, J. Y. Coulter, H. Wang, Q. X. Jia, P. N. Arendt, J. L. MacManus-Driscoll, M. P. Maley, et al., *Applied Physics Letters* **84**, 2121 (2004).
 - ²⁹ P. Berghuis, E. DiBartolomeo, G. A. Wagner, and J. E. Evetts, *Physical Review Letters* **79**, 2332 (1997).
 - ³⁰ J. H. Durrell, S. H. Mennema, C. Jooss, G. Gibson, Z. H. Barber, H. W. Zandbergen, and J. E. Evetts, *Journal of Applied Physics* **93**, 9869 (2003).
 - ³¹ J. H. Durrell, J. E. Evetts, R. Rössler, M. P. Delamare, J. D. Pedarnig, and D. Bäuerle, *Applied Physics Letters* **83**, 4999 (2003).
 - ³² W. F. Hu, X. J. Zhao, W. Peng, T. S. Wang, W. Liu, L. Li, C. Lei, and Y. F. Chen, *Journal of Crystal Growth* **231**, 493 (2001).
 - ³³ L. Mechin, P. Berghuis, and J. E. Evetts, *Physica C* **302**, 102 (1998).
 - ³⁴ U. Poppe, Y. Y. Divin, M. I. Faley, J. S. Wu, C. L. Jia, P. Shadrin, and K. Urban, *IEEE Transactions on Applied Superconductivity* **11**, 3768 (2001).
 - ³⁵ F. Wellhofer, P. Woodall, D. J. Norris, S. Johnson, D. Vassiloyannis, M. Aindow, M. Slaski, and C. M. Muirhead, *Applied Surface Science* **129**, 525 (1998).
 - ³⁶ J. L. Maurice, J. Briatico, D. G. Crete, J. P. Contour, and O. Durand, *Physical Review B* **68**, 115429 (2003).
 - ³⁷ D. H. Lowndes, D. K. Christen, C. E. Klabunde, Z. L. Wang, D. M. Kroeger, J. D. Budai, S. Zhu, and D. P. Norton, *Physical Review Letters* **74**, 2355 (1995).
 - ³⁸ C. Jooss, R. Warthmann, H. Kronmüller, T. Haage, H. U. Habermeyer, and J. Zegenhagen, *Physical Review Letters* **82**, 632 (1999).
 - ³⁹ C. Jooss, R. Warthmann, and H. Kronmüller, *Physical Review B* **61**, 12433 (2000).
 - ⁴⁰ R. Herzog and J. E. Evetts, *Review of Scientific Instruments* **65**, 3574 (1994).

- ⁴¹ M. G. Blamire and J. E. Evetts, Applied Physics Letters **46**, 1181 (1985).
- ⁴² C. J. O. Reichhardt and M. B. Hastings, Physical Review Letters **92**, 157002 (2004).
- ⁴³ C. Carraro and D. S. Fisher, Physical Review B **51**, 534 (1995).
- ⁴⁴ S. A. Grigera, T. S. Grigera, E. F. Righi, G. Nieva, and F. de la Cruz, Physica C **371**, 237 (2002).
- ⁴⁵ J. H. Durrell, M. J. Hogg, F. Kahlmann, Z. H. Barber, M. G. Blamire, and J. E. Evetts, Physical Review Letters **90**, 247006 (2003).